Journal of Intelligent & Fuzzy Systems 43 (2022) 8397–8415
DOI:10.3233/JIFS-221363
IOS Press

A hybrid IMFO-fuzzy algorithm for performance enhancement of microgrid under uncertainty via DGs integration and reconfiguration

Madhumathi Periasamy* and Thenmalar Kaliannan
Department of EEE, Vivekanandha College of Engineering for Women (Autonomous), Tamilnadu, India

AUTHOR COPY

Abstract. Microgrids (MGs) are distributed generation and distribution systems that include distributed generation (DG) units, energy storage systems (ESSs), distributed reactive sources (DRSs), and resilient loads that can operate in either connected or isolated modes. When dealing with uncontrolled DGs such as Wind Energy Systems (WES) and Photovoltaic Energy Systems (PVES), MGs planners have a difficult time making decisions. The work proposed in this paper addresses three interconnected works: (i) the implementation of a rigorous hybrid optimization approach for reconfiguration and DGs placement; (ii) the performance investigation under uncertain behavior of RES-based DGs and demand; and (iii) performance enhancement realization through the replacement of hybrid DGs for RES-based DGs. An Improved Moth Flame Optimization (IMFO), which is a multi-objective optimization method, has been linked with fuzzy logic in order to handle multiple objectives in an efficient manner. These objectives include the minimization of voltage deviation, the reduction of generation cost, and the reduction of loss. The quality of the power, the amount of money saved by consumers, and the benefits to the Distribution System Operator (DSO) might all be improved with the help of a hybrid algorithm. This research is also extended to address the uncertainties of RES-based DGs by replacing hybrid DGs in the most optimal locations. IEEE 33 bus RDS is used to test radial distribution system (RDS) microgrids. For validation purposes, uses 24-hour load patterns to mimic WES and PVES' 24-hour load dispatching behavior. The research findings clearly demonstrate the advantages of microgrids over traditional architectures. The hybrid DG requires an average generating cost of 185.33 $/kW in order to produce 100 kW of power throughout the day with significantly reduced emissions.

Keywords: Renewable energy sources, radial distribution system, optimization, whale optimization algorithm, power loss

Abbreviations

Acronym	Abbreviations
MGs	Microgrids
DG	Distributed Generation units
ESS	Energy Storage Systems
DRs	Distributed Reactive sources
RES	Renewable Energy Sources
PVES	Photovoltaic Energy Systems
WES	Wind Energy Systems
MFO	Moth Flame Optimization
DSO	Distribution System Operator
ES	Energy Storage
RDS	Radial Distribution System
PSO	Particle Swarm Optimizer
OGS	Optimal Generation Scheduling
DFR	Distribution Feeder Reconfiguration
NOs	Normally Open switch

*Corresponding author. Madhumathi Periasamy, Research Scholar,Department of EEE, Vivekanandha College of Engineering for Women (Autonomous), Tamilnadu, India. E-mail: madhumathi9196@gmail.com.

ISSN 1064-1246/$35.00 © 2022 – IOS Press. All rights reserved.

NCs	Normally Closed switch
TEC	Total Emission Cost
TGC	Total Generation Cost
DE	Diesel Engine

Nomenclature

Notations	Description
VD	Bus Voltage Deviation
nb	Total number of load buses present in the system
V_{feeder}	Voltage at the feeder
P_L	Real power Transmission losses
Q_L	Reactive power transmission losses
P_D	Real power Demand
Q_D	Reactive power Demand
$E_{SB}{}^{t.s}$	Stored Energy
E_{SB}^{min}	Minimum Stored Energy
E_{SB}^{max}	Maximum Stored Energy
$P_{SB,ch}^{max}$	Charge Rate
$P_{SB,dis}^{max}$	Discharge Rate
η_{ch}	Charge efficiency
η_{dis}	Discharge efficiency
r_m^{up}	Ramp up
r_m^{down}	Ramp down
Δt	Time period
k_{BOS}	reduction factor
$\mathbf{k_{cloud}}$	the reduction factor due to the clouds present
G_{lum}	global solar irradiance for clear atmospheric conditions
P_{PV_r}	rated power of the PV plant
G_{stc}	global solar irradiance (1000 W/m^2)
V_h	actual wind speed
V_d	cut-in
V_r	rated wind speed of a wind plant
V_w	cut-off
P_{gen}	Real Power Generation
Q_{gen}	Reactive Power Generation
S_{gen}	Apparent Power Generation
I	Current in Iterations
T	Maximum number of Iterations
P_{WT_r}	installed capacity of the wind turbine

1. Introduction

A. General Perspective

The power system is undergoing significant transformations in all areas of design, configuration, operation, and control, as well as many others, in the context of global energy infrastructures. Increased awareness of environmental issues and deregulation of the electricity sector are driving increased demand for distributed generation sources and energy storage systems (ESS), with more and more DG units being accepted and deployed in close proximity to residential areas. Closely located DGs and ESSs provide significant benefits such as increased system dependability, higher energy quality, and lower system loss, power production costs, and environmental pollution, among other things. Although the diversity of this paradigm shift necessitates collaboration and cooperation among distribution and control systems, it also poses certain challenges in the design, operation, and control of energy systems, as illustrated in the diagram below. Power distribution companies face the difficult task of constructing a dependable distribution system that is also cost-effective.

However, when it comes to distribution system economics, one of the most efficient options is reconfiguration, which aims to increase system dependability while also reducing power loss and stabilizing voltage variation.

B. Literature review

Recently, a number of microgrid management techniques, control technologies, and optimization methodologies have emerged, all of which provide strong technological support for microgrids. There is a brief discussion of how intelligent distribution technology has progressed and the developing technologies and future development trends that are being examined in [1]. Several microgrid frameworks are presented using the optimization techniques like adaptive harmony search algorithm [2], Stochastic ranking [3], Benders decomposition [4] cuckoo search algorithm [5] to facilitate energy management, power distribution, DG installation, and renewable energy source allocation. System control, energy storage, power distribution, and market behavior are just a few of the things that can be managed using hierarchical structures defined in [6].

One goal of microgrid energy distribution is to reduce transmission and distribution costs and losses. As described in [7], a hybridization of GWO and the Particle Swarm Optimizer (PSO) reduces power losses in the distribution system by identifying optimal DG size and location, while also taking distribution system restructuring into account. Reference [8] discusses several optimization strategies for RDS

AUTHOR COPY

reconfiguration, DG positioning, and other tasks that reduce power losses in a system. Particle Swarm Optimization (PSO) was used to improve the benefits of microgrid by taking into account factors such as load response and WES uncertainty in [9], where the day-ahead benefit of microgrid is considered the fitness function. In order to reduce the microgrid's overall operating costs while also meeting various utility system operational constraints, an algorithm was also proposed in [10] that would allow the execution of OGS and DFR on a short-term for cast basis. An improved hybrid fuzzy-genetic approach to resolving the problem of network reconfiguration was presented in [11].

Accordingly, the specific parameters and characteristics of the microgrids were used to form the mathematical functions that were then used to establish a model, and then to transform the energy optimization issue into a mathematical problem, as previously stated. A Multi-objective Optimal Dispatch Model of Microgrid (MODMG) was developed using the Interval Optimization (IO) approach, which was then implemented [12]. According to the simulation results based on the enhanced IEEE112 bus MG, the Chaotic Group Search Optimizer with Multiple Producers (CGSOMP) method is useful. One of the main goals of [13] was to reduce the total cost and real power loss of MG while improving convergence speed and better handling operational constraints, in addition to the objective function, which was achieved by using a hybrid optimization technique called Chaotic Binary PSO (CBPSO). Decomposition of economic and emission costs into deterministic problems and then back into the original problem was developed in [14] in an efficient scenario-based stochastic programming technique. To improve the overall performance of this stochastic optimization algorithm, an adaptive probability correction technique was used. Recently, distribution network reconfiguration was conducted in [15] by using DGs to minimize energy loss, THD, and voltage imbalance. [16] designed an energy management technology for the power grid that can handle EV charging and other grid factors. The projected development also sized fast-charging stations on roads with budget in mind. [17] suggested a chance-constrained Distributed Resource Optimization (DRO) issue using microgrids scheduling in connected electrical and gas networks. In order to reduce the overall cost of purchasing electricity from the distribution substation, a planning-operation decomposition technique was established in [18] for the best placement, choice, and operation of BESSs and renewable DGs in medium-low voltage distribution systems. In order to maximize the technical, environmental, and economic benefits, including power loss reduction, voltage profile enhancement, voltage stability conditions improvement, emissions reduction, and annual operational cost decrease, a two-stage multi-objective method was applied in [19]. In [20], a probabilistic approach is used to take into account the demand profile and the intermittent nature of renewable-based DGs. To reduce the cost function of yearly energy loss and annual energy not served, the study examines several annual plans based on the seasonal power profiles of DGs and the load. In order to establish the best timing and capacity for conventional generator units, GB, P2 G, CCHP, and DGs, the paper [21] suggested an affine model for optimal planning of IES taking DG uncertainty and carbon emissions into consideration. The affine model's matrix form was employed to lessen the effect of DG uncertainty. Additionally, suggested was a tiered dynamic charge pricing scheme to lower carbon emissions over the long run of the IES activities. In order to establish the best locations and capacities of various RES-based DGs, BESSs, and CBs in the presence of DR and renewables curtailment, a multi-objective optimization planning model was developed in [22]. The goal of this work was to reduce average power losses in distribution networks while maximizing the economic index and the average voltage stability factor.

The further literature on MG optimization through DG integration and reconfiguration using various optimization approaches is compiled in Table 1. Table 1 shows a comprehensive review of the literature on the subject of solving the microgrid optimization problem using various optimization strategies. The majority of the research in Table 1 has addressed the optimization problem by focusing on finding the optimal DG placement. According to the assumptions made, mathematical model considered, algorithm specific parameters of the optimization technique used, and uncertainty considerations, mathematical complexity is classified into three cases: simple, middle, and complex. As a result of the optimization problem, several studies looked into controllable DGs such as MT, FC, and DE. Emissions from the DGs will unavoidably rise in price over time, making them less cost-effective in the short term. Utilities and their customers are strongly encouraged to generate electricity using renewable energy sources in order to reduce the impact of

AUTHOR COPY

emission costs (RES). Most developing countries must regulate CO2, NO2, and SO2 emissions, which has resulted in the use of renewable energy sources for power generation. Because of their efficiency, longevity, payback period, installation and maintenance costs, and ease of use, wind and solar power are preferred over other renewable sources. Here's a look at the difficulties and uncertainty of producing electricity using two common ES. Several studies, as shown in Table 1, are being conducted in this context, using microgrids and renewable energy sources. Many studies, on the other hand, fail to address the ambiguities associated with WES and PVES. Furthermore, the uncertainties caused by RES have not been adequately addressed in the majority of previous studies. The current work focuses on addressing the issues mentioned above, specifically those related to optimal placement and the solution for the uncertainties of renewable energy sources when integrated into microgrids. It is proposed to solve the distribution system optimization problem in microgrids using a hybrid Fuzzy and MFO method that takes into consideration both the uncertainty of WES and PVES. The prober replacement of hybrid DGs provides a solution for the uncertainties associated with renewable energy sources.

C. Contributions

For reconfigurable microgrids, a hybrid Fuzzy-IMFO approach is developed for determining the optimal DG position. The method is explained in great detail. The following is a list of the proposed work's most significant contributions.

i. Determine the most optimal location of the DGs and the most optimal tie-lines in an interconnected microgrid system, a search strategy based on the IMFO technique is proposed in conjunction with the heuristic fuzzy.
ii. Improvement of CMFO by the incorporation of migration and curvilinear properties in order to improve search capabilities, and heuristic fuzzy is used in conjunction with IMFO to handle multiple objectives at the same time.
iii. Integration of hybrid DGs to replace the RES-based DGs in the optimal locations, resolving the uncertainty behavior of DGs.

Table 1
Comparison of literature

	MT	DE	FC	PV	WT	EV	ESS	VD	Proposed algorithms	Mathematical complexity
[23]		√		√			√	√	Grey Wolf Optimization (GWO) algorithm	Middle
[24]	√		√	√	√	√		√	Depth-First Search (DFS) algorithm	Simple
[25]				√	√			√	Sub-gradient ascent-based distributed algorithm	Middle
[26]	√		√	√	√		√		Particle Swarm Optimization (PSO) algorithm	Middle
[27]				√	√	√	√	√	Genetic algorithm (GA)	Middle
[28]					√			√	Time-varying acceleration coefficients particle swarm optimization (TVAC-PSO) algorithm	Complex
[29]				√				√	Fuzzy Optimization, and Particle Swarm Optimization (PSO) algorithms	Complex
[30]				√	√	√	√	√	Discrete genetic algorithm (DGA)	Simple
[31]	√			√	√	√	√	√	Non-dominated Sorting Genetic Algorithm (NSGAII)	Middle
[32]		√							Genetic Algorithm (GA)	Simple
[33]			√	√	√		√	√	Modified firefly algorithm (MFFA)	Middle
[34]	√		√	√	√		√		Matrix real-coded genetic algorithm (MRC-GA)	Middle
[35]	√		√	√	√		√		Adaptive Modified Firefly Algorithm (AMFA)	Middle
[36]				√				√	Multi-objective Antlion Optimizer (MAO) algorithm	Middle
[37]				√	√			√	Particle Swarm Optimization (PSO)	Simple
[38]	√		√	√	√			√	Multi-objective Genetic Algorithm (MGA)	Middle
[39]				√	√		√		Joint Optimization Approach	Middle
[40]	√	√	√						Moth Flame Optimization (MFO)	Middle

MT: Micro Turbine; FC: Fuel Cell; DE: Diesel Engine; WT: Wind Turbine; EV: Electric Vehicles; ESS: Energy Storage System; VD: Voltage Deviation.

AUTHOR COPY

iv. Evaluation of uncontrolled and hybrid DGs, as well as their realistic components and various combinations

D. Paper organization

The remainder of this work will then be divided into the following sections. Section II delves deeper into the modeling of various DGs and loads. Section III discusses how to build mathematical models that include all of the important goal functions as well as the constraint conditions that go with them. Section IV discusses the main research method as well as the suggested optimization technique. Section V introduces the test system and examines the results of the various case studies. Section VI summarizes the investigation's findings and outlines our proposed research strategy.

2. Modeling of dgs and load data

The usual DG configuration specifics and the demand uncertainty models suggested in this study effort are described in the next subsections. For this, we made use of the equations from [31] and the corresponding parameters.

A. *Uncontrollable DGs*

1) Photovoltaic Energy System Modelling

A photovoltaic (PV) system's energy output is proportional to the amount of irradiance received and the angle at which the light is reflected by the solar PV cell. The weather conditions in the surrounding atmosphere determine the amount of irradiance and the amount of electricity generated by the PV. As a result, it's reasonable to assume that global solar irradiation and photovoltaic generation output are linearly related.

The following statement can be used to calculate the performance of a photovoltaic system:

$$P_{PV_{lm}} = k_{cloud} \cdot k_{BOS} \cdot \frac{G_{lum}}{G_{stc}} \cdot P_{PV_r} \qquad (1)$$

Where, kcloud. represents the reduction factor due to the presence of clouds, kBOS.represents the reduction factor that considers the physical infrastructure of the PV system other than the photovoltaic panels (wiring, switches, solar inverter) in real-time operation, Glum represents the global solar irradiance for clear atmospheric conditions in a specific hour of a generic day in the year, Gstc represents the global solar

A solarimeter or pyranometer is frequently used to determine the amount of solar radiation received by the system. Because of the relative geometry of cloud propagation in a PV system, it is necessary to comprehend this geometry in order to compute the photovoltaic system's power output correctly. Some assumptions are made in order to reflect the many scenarios that ptovoltaic plants face. For example, it is assumed that on overcast days, the total solar irradiance will be reduced b90%, and that shade will reduce the total solar irradiance by 50%.

T overall cost of generating per kW is calculated by adding up the expenses of installation, operation, and maintenance for the plants, regardless of whether the PV plant's operating costs are low in comparison to other types of power plants. PVES's generation cost functions are written as follows:

$$PVES_{cost,i} = c^{g}_{PVES,i} * \left(\frac{C_{PVES,In,i}}{K_{PVES,i}} + C_{PVES,OM,i} \right) \qquad (2)$$

Where $c^{g}_{PVES,i}$ is an installed capacity of i-th PVES, KPVES, i is a designed lifetime of i-th PVES, $C_{PVES,In,i} and C_{PVES,OM,i}$ represent respectively the installation, and operation and maintenance cost of the i-th PVES.

2) Wind Energy System Modeling

In wind farms, power production is reliant on the availability of utility services, which may change with regard to time; wind energy generation is greatly impacted by seasonal and regional variations, as well as by time of day and year. While doing so, it is necessary to take into account extremely short-term variations, which is difficult to do in a distribution system that has shortcomings. The power generated by the WES may be calculated by taking the time series of the main power supply, which is written as (3),

$$P_{WT_h} = \begin{cases} 0 & 0 \le v_h \le v_d \\ P_{WT_r} \frac{v_h - v_d}{v_r - v_d} & v_d < v_h < v_r \\ P_{WT_r} & v_r \le v_h \le v_\omega \\ 0 & v_h > v_\omega \end{cases} \qquad (3)$$

Here, v_d, v_ω and v_r are the cut-in, cut-off and rated wind speed of a wind plant, respectively, v_h is the actual wind speed, and P_{WT_r} is the installed capacity of the wind turbine.

AUTHOR COPY

The generation cost of a wind energy system can be evaluated ung the following expression (4), just like the PVES.

$$WES_{cost,i} = c^{g}_{WES,i} * \left(\frac{C_{WES,In,i}}{K_{WES,i}} + C_{WES,OM,i} \right) \tag{4}$$

B. *Demand uncertainty*

Because the power system is dynamic, it gets increasingly difficult to anticipate and estimate load characteristics over time as the system becomes more complex. In any case, accurate load estimates are more crucial than ever for selecting the most efficient operation. In this study, the probability Density Function (PDF) taken from [44] is used to simulate the change in load on the power system, which may be stated as follows:

$$f^{l}_{i,t} = \frac{exp\left[\frac{p_{i,t} - \mu^{l}_{i,t}}{2\left(\sigma^{l}_{i,t}\right)^{2}} \right]}{\sqrt{2\pi\sigma^{l}_{i,t}}} \tag{5}$$

where,

$$\mu^{l}_{i,t} = \frac{\sum_{j=1}^{n} p_{i,t,j}}{n_{i,t}} \tag{6}$$

$$\sigma^{l}_{i,t} = \frac{\sum_{j=1}^{n} \left(p_{i,t,j} - \mu^{l}_{i,t} \right)}{n_{i,t} - 1} \tag{7}$$

3. Mathematical formulation of the problem

A. Objective functions

In order to address the issue, we used two objective functions:he total generation cost minimization function and the bus voltage deviation reduction function.

1) Minimization of Total Generation Cost

The utilization of restructure and appropriate DG placement we used in this research in order to achieve optimization. Therefore, the total generation cost (TGC) minimization is defined as a function of the expenses associated with the grid, WES, and PVES. Minimize

$$TGC = Grid_{cost} + \sum_{i=1}^{nWES} WES_{cost,i} + \sum_{i=1}^{nPVES} PVES_{cost,i} \tag{8}$$

Where nWES and nPVES represent the total number of WES and PVES installed in the microgrid, respectively.

Cost function of grid:

$$Grid_{cost} = P_{grid} * K_{grid} \tag{9}$$

Where K_{grid} represents the cost co-efficient constant and assumed as 44 $/W-hr. $WES_{cost,i}$

And $PVES_{cost,i}$ are the generating cost of i-th WES and PVES, respectively.

2) Minimization of bus voltage deviation

The reduction of TGC is considered an extra goal in addition to the reduction of bus voltage fluctuation in order to assure operational security and voltage quality to the client ends. The minimal bus voltage fluctuation with respect to the supplied reference voltage is stated as follows for all of the system's load buses:

$$VD = \sum_{i=1}^{nb} |V_i - V_{\text{ref}}| \tag{10}$$

In the above equation (10), V_{ref} is the reference voltage, V_i is the i-th bus voltage and 'nb' refers the load buses present in the system.

B Operational constraints

In order to solve this optimization problem, a number of equality and inequality constraints are taken into account, as detailed in the following subsections.

This optimization problem has several constraints.

1) Equality Constraints

The constraints for power balance requirements:

$$\sum_{i=1}^{NG} PG_i - P_L = P_d \quad \sum_{i=1}^{NG} QG_i - Q_L = Q_d \tag{11}$$

2) Inequality constraints

a. Generator Operation Constraints

The generating units' power generation should be kept within the range.

$$\max\left(P_i^{min}, P_i^0 - DR_i\right) \le P_i \le \min\left(P_i^{max}, P_i^0 + UR_i\right) \tag{12}$$

and

$$P_i \in \begin{cases} P_i^{min} \le P_i \le P_{i,1}^{l} \\ P_{i,j-1}^{u} \le P_i \le P_{i,j}^{l} \ , j = 2, 3, ..., n_i, i = l, ..., m. \\ P_{i,n_i}^{u} \le P_i \le P_i^{max} \end{cases} \tag{13}$$

AUTHOR COPY

b. Line Flow Constraints

The active, reactive and apparent power restrictions of elecical per equipment's are expressed in equations (16)–(18).

$$\leq P_{G_i}^{max} \quad 1 \leq i \leq N_G \tag{14}$$

$$Q_{G_i}^{min} \leq Q_{G_i} \leq Q_{G_i}^{max} \quad 1 \leq i \leq N_G \tag{15}$$

$$|S_k| \leq S_k^{max} \quad 1 \leq k \leq N_G \tag{16}$$

c. Bus voltage limits

$$0.95 \leq Vi \leq 1.05, i = 1, 2, ..., nb \tag{17}$$

d. DG Power factor limit

$$0.8 \leq PF \leq 1 \tag{18}$$

e. DG Limits

The real and reactive power handling capacities of the DG units are given below:

$$0 \leq P_{\text{gen},i,max} - P_{\text{gen},i,s} \perp \frac{1}{m_{p,i}} \left(\omega_i^* - \omega_s\right) - P_{\text{gen},i,s} \geq 0, \forall i \in N_{\text{droop}} \tag{19}$$

$$0 \leq Q_{\text{gen},i,max} - Q_{\text{gen},i,s} \perp \frac{1}{n_{p,i}} \left(|V_k|^* - \left|V_{k,s}\right|\right) Q_{\text{gen},i,s} \geq 0, \forall i \in N_{\text{droop}} \tag{20}$$

From the real and reactive power handling limits, the apparent power handling limits can be obtained as given below:

$$\sqrt{\left(P_{\text{gen,i,s}}\right)^2 + \left(Q_{\text{gen,i,s}}\right)^2} \leq S_{\text{gen,i,max}}, \quad \forall i \in N_{\text{droop}} \tag{21}$$

4. Proposed search strategy

The two technologies used in the suggested work, IMFO and heuristic fuzzy, are described in this section. In order to handle multiple objectives, fuzzy is integrated with IMFO to find the best solution. Before dealing with the IMFO, the classical MFO concept is briefly explained for better comprehension.

A. Classical Moth Flame Optimization (SMFO)

The Moth-flame Optimization (MFO) method [41] was created by Seyedali Mirjalili and is a groundbreaking population-based strategy inspired by natural phenomena and grounded in the principles of evolutionary computing. The fitness values for each population in each iteration are determined by randomly generated variables, and the MFO method uses moths to represent tse values and flames to represent the best solutions at the end of each iteration.

The moths may be thought of as a matrix, as follows:

$$M = \begin{bmatrix} M_{1,1} & M_{1,2} & \cdots & M_{1,d} \\ M_{2,1} & M_{2,2} & \cdots & M_{2,d} \\ \vdots & \vdots & \cdots & \vdots \\ M_{n,1} & M_{n,2} & \cdots & M_{n,d} \end{bmatrix} \tag{22}$$

The number of moths and the problem's control variables are represented by 'n' and 'd,' respectively. As a result, the individual moths' fitness values form an array that looks like this:

$$OM = \begin{bmatrix} OM_1 \\ OM_2 \\ \vdots \\ OM_n \end{bmatrix} \tag{23}$$

The n-th moth's fitness value is represented by the term OMn in the equation above. The structure of flames is similar to that of moths, and can be summarized as:

$$F = \begin{bmatrix} F_{1,1} & F_{1,2} & \cdots & F_{1,d} \\ F_{2,1} & F_{2,2} & \cdots & F_{2,d} \\ \vdots & \vdots & \cdots & \vdots \\ F_{n,1} & F_{n,2} & \cdots & F_{n,d} \end{bmatrix} \tag{24}$$

Arrays are used to store the corresponding fitness values for the flames.

$$OF = \begin{bmatrix} OF_1 \\ OF_2 \\ \vdots \\ OF_n \end{bmatrix} \tag{25}$$

For each nth flame, the fitness value is stored in the variable OFn. When addressing the non-linear prob-

AUTHOR COPY

lem, the MFO algorithm uses a unique 3-dimensional approach, expressed as, to obtain convergence.

$$MFO = (I, P, T) \tag{26}$$

There are a number of random moths and their fitness levels recorded in the function "I." Function 'P' keeps track of a moth's last known location inside a search area.ver talting conditions are reached, function "T" shuts off the solution process.

This method uses a logarithmic spiral to track the journey of moths.

$$S\left(M_i, F_j\right) = D_i e^{bt} cos\left(2\pi t\right) + F_j \tag{27}$$

$$D_i = \left|F_j - M_i\right| \tag{28}$$

Where D_i represents the distance of i-th moth with respect to j-th flame, 'b' is a co-efficient of the logarithmic spiral and $t \in (-1, -2)$.

During iterations, the number of flames is decreasing gradually to enhance the detection of the optimal solution:

$$flameno = round\left(n - l\frac{n-1}{T}\right) \tag{29}$$

Where '*l*' and '*T*' represents the current and maximum iterations, respectively.

In MFO, all jobs are depicted as moths that flutter around in search space, always adjusting their position according on their own and the flames' own experiences. The priorities of each moth are used to determine if work should be sent to a private cloud or an EC, as indicated. MFO aims to distribute cloud resources more efficiently by employing a moth (a collection of priorities). There are two factors that boost the search capacity: the logarithmic spiral adaptation and the progress updates of the moths' positions in relation to other moths.

B. Improved MFO (IMFO)

Because of its inability to cope with a wide range of problems, classical MFO has been avoided in scientific and technical fields. If the task at hand is very challenging, it is possible to get bogged down in local optimal. A solution to the VM allocation problem isn't as simple as it appears at first.. Because of this, a stronger and more resilient MFO is needed to successfully tackle this issue. Increasing the variety of moths and flames can help avoid local optimization. MFO is used in conjunction with a migrating and descending curve [45] to keep track of the location of flames and moths.

1) Migration principle

By producing a new, diverse moth population from scratch, this method eases the burden of sifting through a limited supply of moths. A new generation of moths is born on the basis of the best individual $N_{i,b}$. An individual's moth gets converted into the following in this case:

$$N_{i,d} = \begin{cases} N_{i,b} + \alpha_{i,d}\left(N_{d,min} - N_{i,b}\right) if_{i,d} < \frac{N_{i,b} - N_{d,min}}{N_{d,max} - N_{i,b}} \\ N_{i,b} + \alpha_{i,d}\left(N_{h,max} - N_{i,b}\right) otherwise \end{cases} \tag{30}$$

There are two random numbers in this equation: one is called, -i,d. and the other is, -i,d. As a result, the first selection parameters are based on this heterogeneous population. It is only possible to migrate if moth population density (ρ) is less than a tolerance for moth population diversity (ε_1), as shown in expression (31) of the equation for migrating.

$$\rho = \frac{\sum_{i=1}^{n} \sum_{h=1}^{d} \eta_z}{\substack{i \neq b \\ d\,(n-1)}} < \varepsilon_1 \tag{31}$$

Where

$$\eta_z = \begin{cases} 1 if \left|\frac{N_{i,d} - N_{i,b}}{N_{i,b}}\right| > \varepsilon_2 \\ 0\ otherwise \end{cases} \tag{32}$$

Aindex of the moth diversity relative to the best individual is denoted by. There is no end in sight to the cycle until there is no progress in the best person. An integer variable rerred to as "n" is used in equation (32), where "b" refers to the position of the best moth, while "h" and "d" are the integer variables that represent the creation of the best moths.

2) Descending curvilinear principle

This concept has been reworked in order to speed up the process of finding the optimal answer. Moth swarm behavior has a huge number of random states, which means that an algorithm that is very time-consuming is required. By switching from a linear (21) to a curved descent updating process, the adaptive flame number and the algorithm's convergence

AUTHOR COPY

speed can be improved. Adaptive flames are counted according to this new methodology.

$$flameno = round\left(\frac{T}{l+\left(\frac{T}{n}\right)}\right) \tag{33}$$

The pseudocode of the proposed IMFO algorithm is detailed below.

Input: Maximal iteration number (MAXIT), Number of Control variables (d)
Number of Moths (n), iterCount = 0
Output: OptimalSolution
//Execute the following steps if (iterCount < MAXIT)
{
//Preparation phase of Moths
M(n,d)=random()
Obj(M(n))
//Preparation phase of Flames
F(n,d)=random()
Obj(F(n))
// interaction phase of Moths and flames
D = f(F,M)
// updation phase of Moths
S = f(F,M)
M = f(S)
finalM = best(M)
// Migration operation
M = f(finalM)
// limiting the flow of flames for further iterations
F = f(n,l,T)
iterCount = iterCount+1
}
Display finalM

The flowchart in Fig. 1 depicts the step-by-step process flow of the MFO algorithm.

C. Heuristic Fuzzy

The total generation cost (TGC) and the voltage deviation (VD) are the two objective functions to be minimized in this problem. In order to establish a middle, ground between these two goals, the heuristic fuzzy technique has been used. A wide range of decision-making latitude is provided by the use of flexible membership functions with maximum and minimum limits for each fitness function. The fuzzy functions that have been built can be changed to better match the needs of the issue based on the contributions of the fitness functions. Detailed explanations of the two aim functions will be provided in subsequent sections.

1) Membership Function for TGC

There have been suggestions that the solution's whole production cost be kept to a minimum. GCfactor is therefore defined as the ratio of total generation

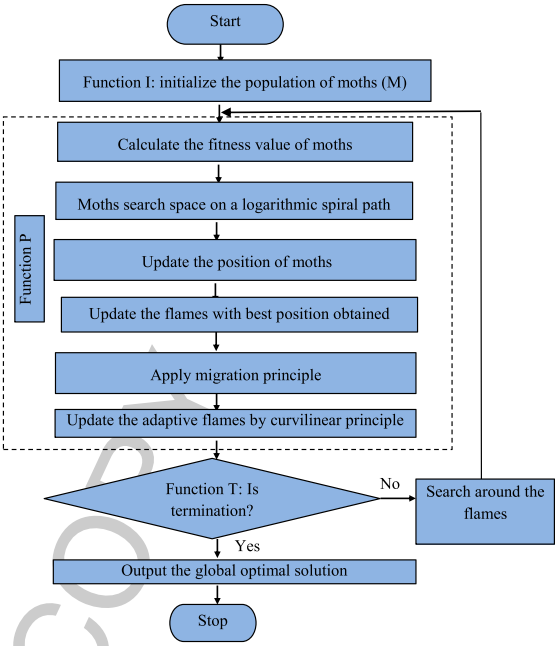


Fig. 1. The flow chart of the IMFO algorithm.

costs after and before optimization at a certain load level.

$$GC_{factor} = \frac{TGC_{\text{after}}}{TGC_{\text{before}}} \tag{34}$$

In (38), the solution gets the maximum benefit for the lower values of GC_{factor}. The membership function is expressed as,

$$\mu_{TGC} = \begin{cases} 1, GC_{factor} \le GC_{\min} \\ \frac{GC_{\max} - GC_{factor}}{GC_{\max} - GC_{\min}}, GC_{\min} < GC_{factor} < GC_{\max} \\ 0, GC_{factor} \ge GC_{\max} \end{cases} \tag{35}$$

In this work, $GC_{\min}$ and $GC_{\max}$ are assumed with the values 0.5 and 1, respectively.

2)Membership Function for VD

The voltage limit at the buses is the most sensitive operational restriction of the system when it is powered by distributed energy sources. The reduction of bus voltage variation is being explored in conjunction with the primary goal in order to overcome this problem. New populations cause the system's minimum bus voltage to be reached, and this voltage is logged as VDafter in the system's log. In order to calculate the voltage deviation factor (VDfactor), the voltage deviation factor (VDafter) and the minimum

AUTHOR COPY

bus voltage in the initial setup are taken into account (VDbefore) which is expressed as follows:

$$VD_{factor} = \frac{VD_{after}}{VD_{before}} \tag{36}$$

The membership function for the population can be expressed as follows,

$$\mu_{VD} = \begin{cases} 1.0, VD_{factor} \leq VD_{min} \\ \frac{VD_{max} - VD_{factor}}{VD_{max} - VD_{min}}, VD_{min} < VD_{factor} < VD_{max} \\ 0.0, VD_{factor} \geq VD_{max} \end{cases} \tag{37}$$

In the above equation, VD_{min} and VD_{max} are considered as 0.05 and 0.1, respectively. The choice fuzzy set (38) is used to find a compromise solution between the two membership functions defined in (35) and (37).

$$\mu D = min(\mu TGC, \mu VD) \tag{38}$$

The decision fuzzy set is considered as the fitness function for MFO, and it has been assessed with each new arrival of the population in the MFO population. The proposed algorithm is written in MATLAB and executed on an Intel Core i5 processor with a clock speed of 4.1 GHz, as shown in Fig. 1.

5. Simulation and results

A. Test system data and DGs parameters

The investigation in this work is focused on the IEEE 33 bus RDS (Radial Distribution System), which is depicted as a single line diagram in Fig. 2.

Table 2
IEEE 33 bus system parameters

Parameters	Values
Base kV	12.66 kV
Base MVA	100 MVA
Total real power loading (P_d)	3.715 MW
Total reactive power loading (Q_d)	2.3 MVAR
Initial configuration real power loss (P_L)	202.66 kW
Maximum Current Capacity of the branches (I_{br})	400 A
Minimum bus voltage limit (V_{min})	0.9 pu
Normally Open switches (NO's)	S_{33}, S_{34}, S_{35}, S_{36}, and S_{37}
Normally Closed switches (NC's)	S_1 to S_{32}

Table 3
Characteristic data of PVES and WES

Parameters	Definition	Energy system	
		PVES	WES
Life Time	K	20	12.5
Installation Cost ($/kW)	C_{In}	7000	2500
Depreciation Time (in years)	C_{om}	20	10
Depreciation Cost ($/kW-year)	–	712.92	372.57
Installed Capacity (kW)	C_g	100	100

This system is made up of 37 branches, each of which has a switch, as well as 33 buses. Table 2 has a full overview of the system's configuration. [32] contains the test system's characteristic data, as well as line and load statistics.

In this study, it will be investigated how the impact of WES and PVES on the reconfigurable microgrid may be decreased. Table 2 depicts the characteristics of the two energy systems under examination. Figure 3 depicts the hour-to-hour efficiency considerations for the WES and PVES. [39] is used to provide more detailed information about energy systems.

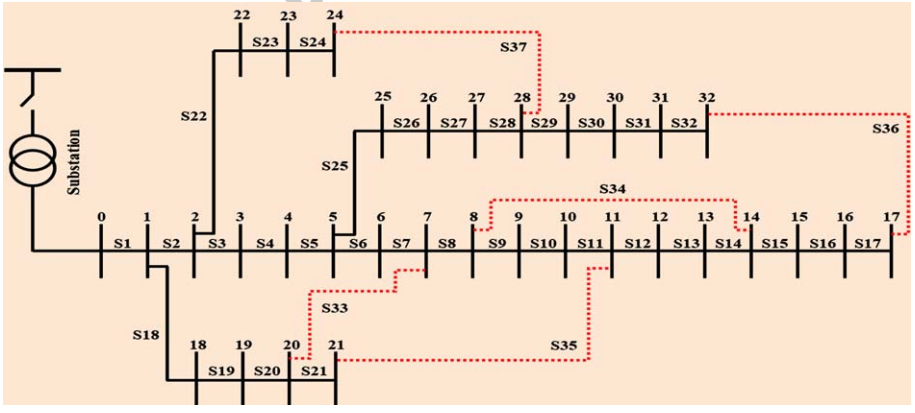


Fig. 2. Single-line diagram of IEEE 33 Bus RDS.

AUTHOR COPY

Table 4
Set of switches in each zone

Zone (Z)	Normally Closed Switches (NCs)	Normally Open Switches (NOs)
1	$\{S_4, S_5, S_6, S_7, S_{19}, S_{20}\}$	$\{S_{33}\}$
2	$\{S_{12}, S_{13}, S_{14}\}$	$\{S_{34}\}$
3	$\{S_8, S_9, S_{10}, S_{11}, S_{21}\}$	$\{S_{35}\}$
4	$\{S_{15}, S_{16}, S_{17}, S_{29}, S_{30}, S_{31}, S_{32}\}$	$\{S_{36}\}$
5	$\{S_{23}, S_{24}, S_{25}, S_{26}, S_{27}, S_{28}\}$	$\{S_{37}\}$

The importance of RES placement in this research is due to the fact that it involves both reconfiguration and placement of RES in the most appropriate spot. The identical procedure for reconfiguration operation was used in all of the above-mentioned test cases. The active zones must be ready before an RDS can be updated. Given the significance of tie-switches in the restructuring process, the active zone of a system is defined by the number of habitually open switches in the system. This is due to the test system's five tie switches, which correspond to active zones in the simulation. This is due to the test system's five tie switches, which correspond to active zones in the simulation. When the five distinct zones are seen as solution sets, it is claimed that the number of switches present in each zone reduces. The iterative technique, on the other hand, may help to avoid the selection of improbable solution sets. During the iterative phase, the system switches are categorized based on their position to eliminate implausible solution sets and boost the efficiency of the optimization process [40]. Table 4 displays the complete list of switches for each zone. In this test example, each zone is considered as a microgrid, resulting in a total of five microgrids that are all linked.

B. Performance Investigation of Microgrid with the Presence of WES

The performance of a microgrid in the presence of only WES in the RDS was evaluated in this test scenario, and the findings were determined to be good. The research ised on the assumption that only five WES are permitted to join to the microgrid. As a result, the proposed hybrid technique preserves five variables for reconfiguration and another five variables for identifying the optimal position of WES within the microgrid. As a result, a total of 10 control variables and their cresponding ranges are used for optimal searching via IMFO, with fuzzy decision set (39) serving as the fitness function. Using the provided approach, 50 iterations and 50 populations are performed. Following a successful test, bus numbers 31 and 32 were selected as the best locations for WES installation. The ideal configuration's recognized NOs are S7, S9, S14, S32, and S37. The convergence characteristics of the firefly algorithm (FFA) [33] and particle swarm optimization (PSO) [37] are compared with the classical and improved MFO to assess the utility of the suggested approach when the algorithms are run with the same iteration and population values. The convergence of the researched objectives, such as TGC and VD, is depicted separately in Figs. 4 and 5. The figures show that the proposed method reaches the optimum solution after 29 iterations, displaying better convergence than other two algorithms and classical MFO. Furthermore, it has arrived at a solution that is extremely close to optimal by the 20th iteration. More specifically Fig. 4 reveals that the IMFO generates the best solution of 194.68$/hr, which is superior

AUTHOR COPY

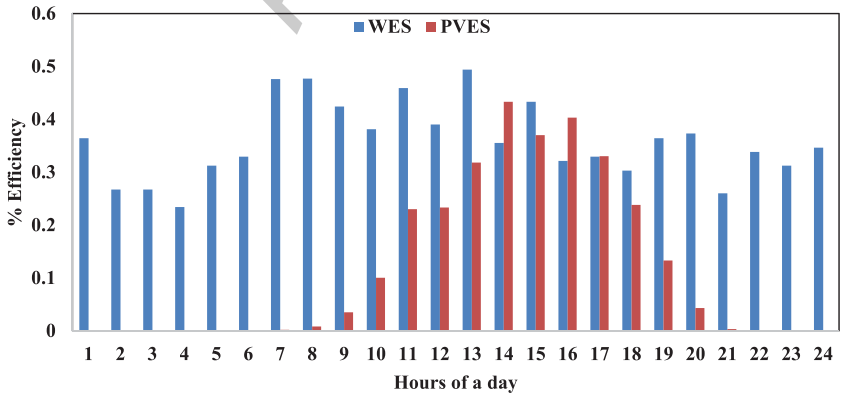


Fig. 3. Percentage efficiency of ES in a day.

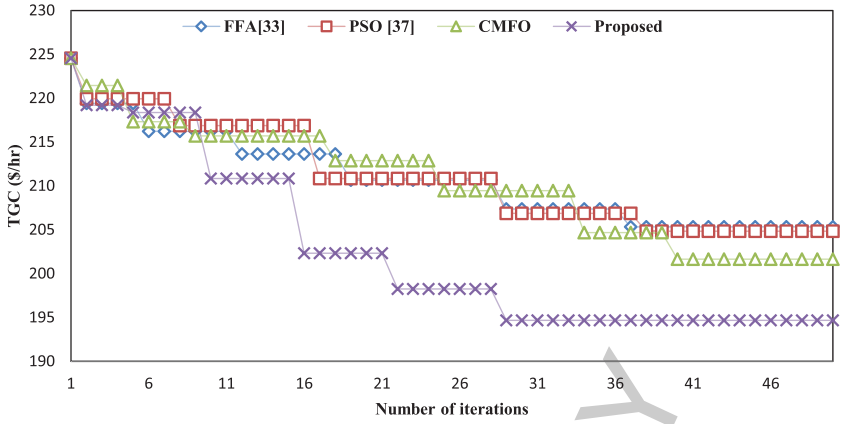


Fig. 4. Convergence of the Different Algorithms for TGC.

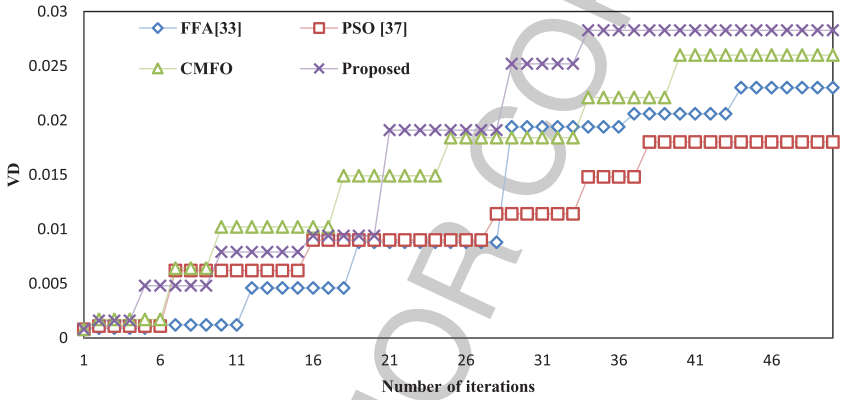


Fig. 5. Convergence of the Different Algorithms for VD.

to the results produced by the FFA of 205.32$/hr, the PSO of 204.83$/hr, and the CMFO of 201.64$/hr. In terms of the voltage deviation index, Fig. 5 shows that IMFO outperforms the other three algorithms, including CMFO.

C. Performance Investigation of Microgrid with the Presence of PVES

This test case is run under the assumption that PVES are present in the microgrid under examination. Only five PVES were available for electricity generation, as was the situation in the previous test instance. The same boundary conditions as in the previous case are utilized to optimize the hybrid approach as in the previous example. Table 3 summarizes the features that set the PVES apart from other systems. Following the successful implementation of the suggested approach, the optimum solution was determined on the process's 33rd iteration. The PVES microgrid findings have been compiled. The power loss of the system is decreased from 202.66 kW to 108.67 kW, with a total generation cost of 235.06$/hr and a minimum bus voltage of 0.9476 observed at bus 32. The ideal PVES position and configuration are the same as in the previous scenario. The bus voltages and branch currents produced from the best design are compared to those obtained from the other system configurations, as shown in Figs. 9 and 10 of the system. As seen in the figures, the bus voltages are higher and the branch current loading is lower in contrast to the other two designs.

D. Performance Investigation of Microgrid with varying DG penetration

In this section, the electrical and nonelectrical features of DGs were examined by altering the number of WES and PVES between 1 and 10 independently. Iteration and population values are set to 50 and 50, respectively, to achieve the same results under the same conditions. For comparison, a simulated result with and without DG deployment is provided.

AUTHOR COPY

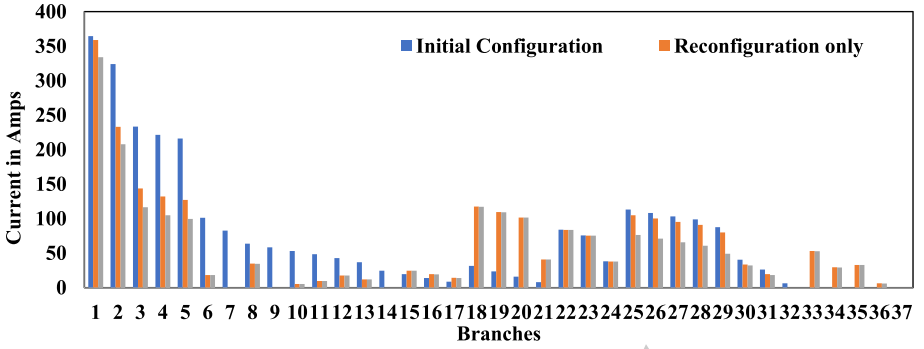


Fig. 6. Comparison of branch currents with PVES under different configurations.

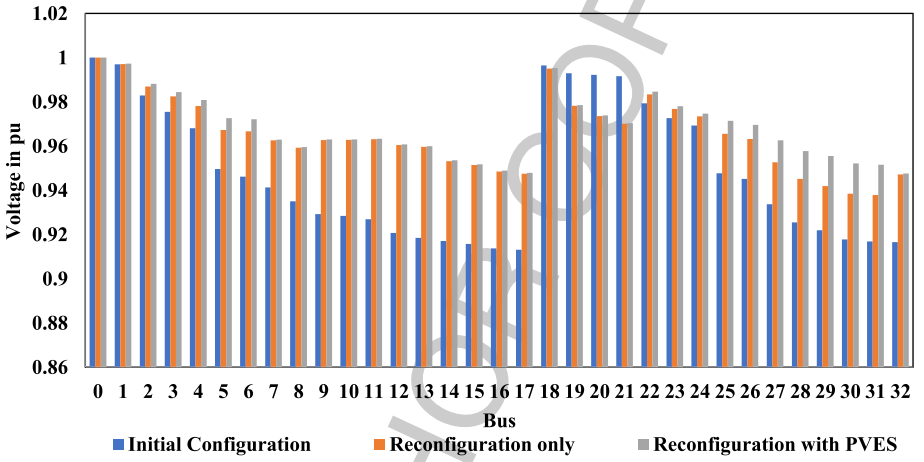


Fig. 7. Comparison of bus voltages with PVES under different configurations.

AUTHOR COPY

1) WES with varying DG penetration

As depicted in Fig. 3, the WESs are uncontrollable generation units that are highly reliant on environmental circumstances, and the model employed in this study is assumed to operate at rated power of 0.01 MW/h throughout the time zone 9 on the graph. Table 5 shows the greatest results achieved by integrating various numbers of WES.

As shown in Table 5, the system configuration remained steady as the number of WES users rose. The cost of power generation is progressively rising from 169.60 $/hr to 186.34 $/hr due to high installation and maintenance expenses; however, the power transmission loss is decreased by 41.33 percent to 81.86 kW/hr, and the minimum bus voltage is raised to 0.9508 pu. Most importantly, the system's emissions are greatly decreased as a result of WES's rising contribution to power production.

2) PVES with varying DG penetration

This research is carried out with varied quantities of PVES penetration in the system, as shown in the figure. PVESs, like wind turbines, are volatile generating units that are heavily influenced by environmental conditions. Because of the ease with which this may be accomplished, we will assume that the rated power of the PVES is 0.1 MW/hr and that it operates in time zone 9 of the characteristics graph shown in Fig. 3. Table 6 displays the simulated consequences for various amounts of PVES penetration based on the simulation parameters.

Table 6 shows how goal values have changed over time as the number of PVESs deployed has increased. PVES has not resulted in a significant change in the system configuration, as it did with WES. The cost of energy production has increased by 43.56 percent to 243.4775 dollars per hour, while

Table 5
Optimal solution under increasing WES penetration

No. of WES	Optimal Configuration	Total Cost in $/hr	Power Loss in kW	Min Voltage in pu.	Bus Number
0	7,9,14,32,37	169.60	139.54	0.9378	31
1	7,9,14,31,37	171.16	131.40	0.9317	31
2	7,9,14,31,37	172.68	122.11	0.9391	31
3	7,9,14,31,37	174.28	114.49	0.9466	31
4	7,9,14,31,37	176.02	110.29	0.9471	31
5	7,9,14,30,37	177.65	103.56	0.9409	30
6	7,9,14,30,37	179.32	97.63	0.9480	30
7	7,9,14,30,37	181.10	94.30	0.9431	30
8	7,10,14,28,30	182.89	91.23	0.9447	30
9	7,9,14,30,37	184.57	85.45	0.9529	30
10	7,9,14,30,37	186.34	81.87	0.9508	30

Table 6
Optimal solution under increasing PVES penetration

No. of WES	Optimal Configuration	Total Cost in $/hr	Power Loss in kW	Min Voltage in pu.	Bus Number
0	7,9,14,32,37	169.60	139.54	0.9378	31
1	7,9,14,31,37	176.87	131.40	0.9317	31
2	7,9,14,31,37	184.10	122.11	0.9391	31
3	7,9,14,31,37	191.39	114.49	0.9466	31
4	7,9,14,31,37	198.77	108.61	0.9503	30
5	7,9,14,31,37	206.23	104.69	0.9518	30
6	7,9,14,30,37	221.04	94.29	0.9477	30
7	7,10,14,31,37	221.07	94.88	0.9545	30
8	7,10,14,30,37	228.42	88.46	0.9500	30
9	7,10,14,28,30	235.92	85.54	0.9530	30
10	7,10,14,31,37	243.47	83.58	0.9544	31

the power transmission loss has decreased by 40.10 percent to 83.58 kW/hr, and the minimum bus voltage has improved to o.9544 volts per hour, according to objective data. PVES integration, like WES integration, has a significant influence on emissions reduction, with a decrease of 27.40 percent.

E. Performance Investigation of Microgrid with the Presence of WES and PVES

The purpose of this test scenario is to determine the capacity of various combinations of WES and PVES to generate energy while a total of five ES are limited for power production. An optimization was performed using the provided technique with a population size of 50 and a maximum number of iterations of 100. The equivalent efficiency of WES and PVES in a given hour under a variety of load demands throughout the day is considered in this research. The suggested hybrid algorithm finds the optimal solution for all feasible combinations of situations. Under a range of load circumstances, the best results are obtained with various combinations of WES and PVES. Figures 8, 9, and 10 illustrate the microgrid's actual power loss, the microgrid's overall manufacturing cost, and the microgrid's minimal bus voltage, respectively. The investigations yielded the following conclusions:

a. When the number of WES is increased, the overall system generation cost and real power loss decrease, as the generation cost of WES is less than that of PVES, resulting in a decrease in both.
b. PVES generates no electricity for around 12 hours per day and reaches a power generation efficiency of more than 25% for only 8 hours per day. PVES, on the other hand, would fare better in the warmer months than WES.
c. When the WES's daily efficiency is compared to the PVES's, the WES is more efficient.
d. PVES, on the other hand, can be installed everywhere because it is not subject to any unique environmental requirements, whereas WES installation is restricted to locations with an appropriate wind velocity.

F. Hybrid PV-DE and WES-DE integrated with microgrid

As demonstrated by the previous cases, the efficiency of the RES is considered a major issue when it

AUTHOR COPY

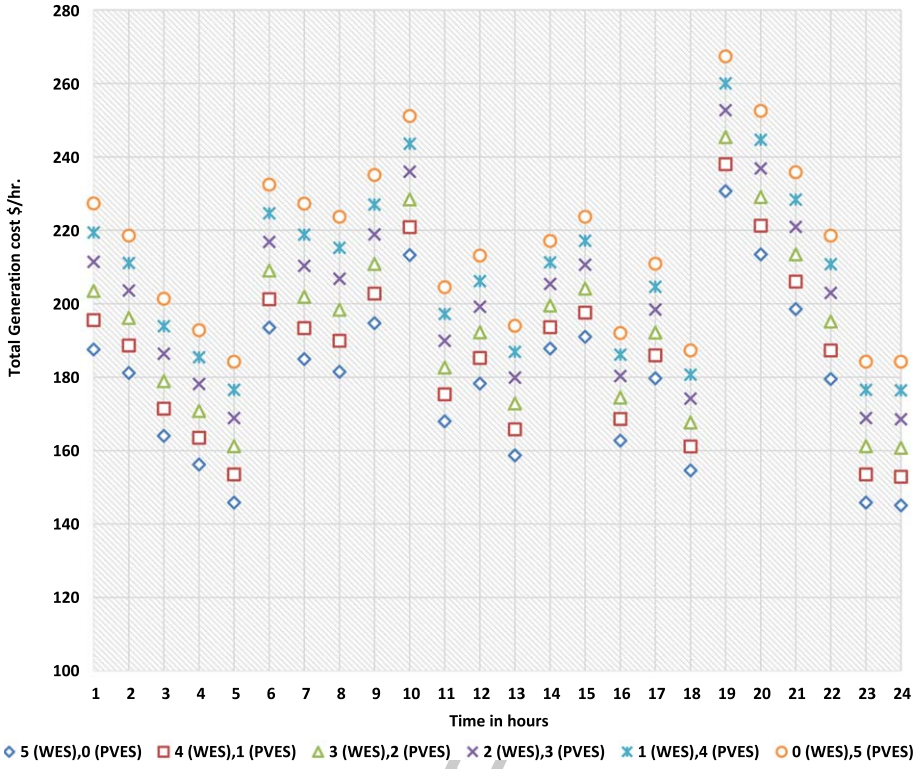


Fig. 8. TGC under varying load conditions with different load sharing by WES and PVES.

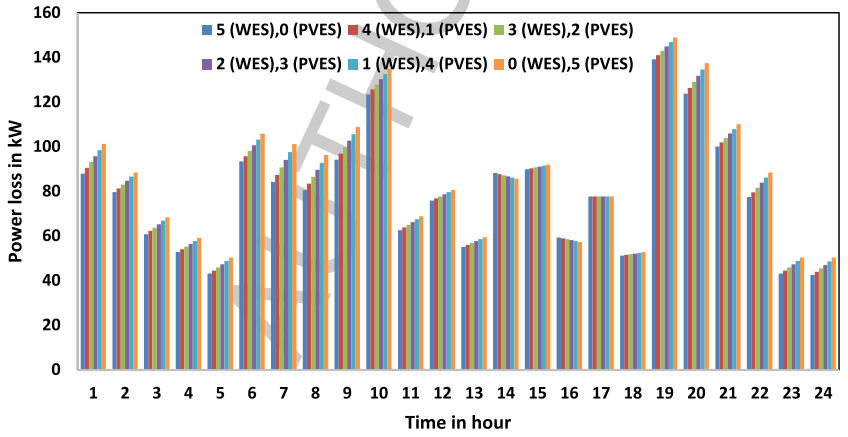


Fig. 9. Power loss under varying load conditions with different load sharing by WES and PVES.

is linked to the microgrid. Only 25% of the day is used by PVES, which means that it is powerless for about 12 hours a day. Summertime PVES would be far more efficient than wintertime WES. It is necessary for the installation to have an appropriate wind speed at all times of the day in order to meet WES requirements. Despite the fact that the RES are installed in the best possible locations, their overall delivery performance is below par. Because of climate change and depletion of traditional energy sources, renewable energy is the best option. RES's advantages as a performance enhancer have been preserved thanks to these factors. A large number of studies involving hybrid DGs have been completed recently. The hybrid DG consists of controllable DGs and renewable energy sources, and it ensures a steady power

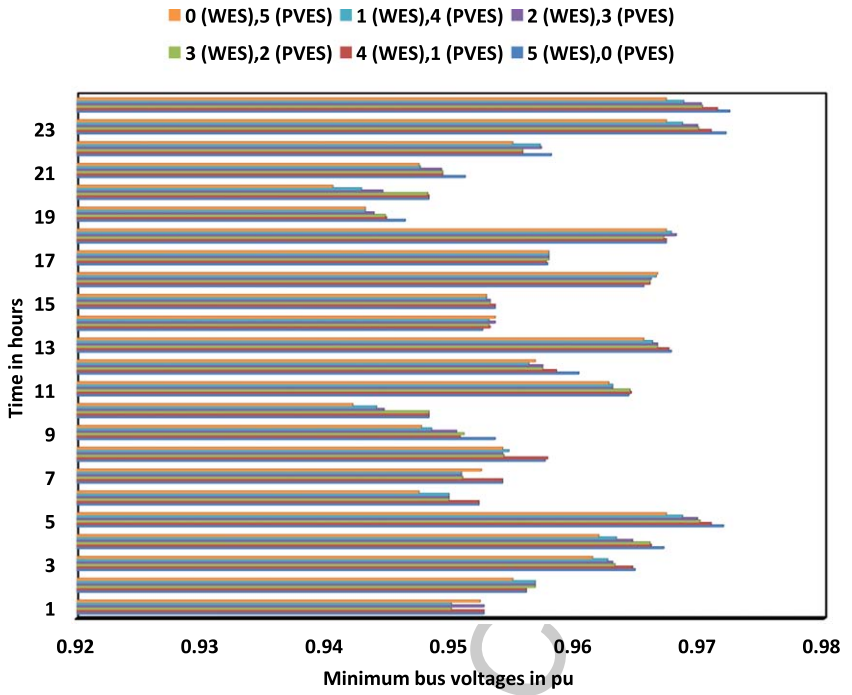


Fig. 10. VD under varying load conditions with different load sharing by WES and PVES.

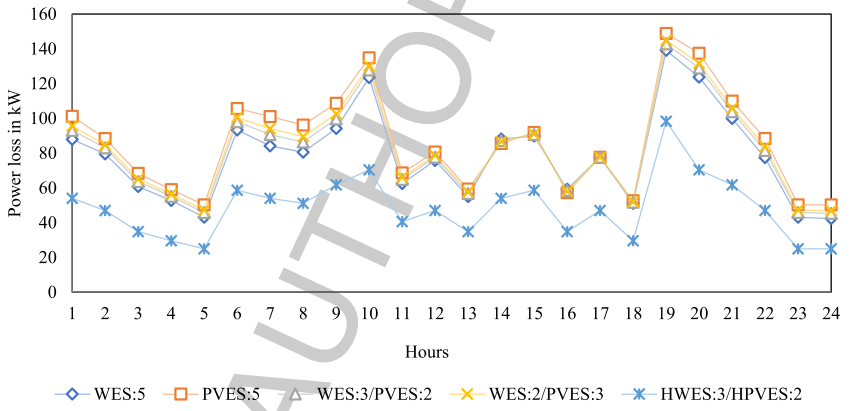


Fig. 11. Power loss under different configurations of microgrid.

supply at the Point of Common Coupling (PCC). The use of controlled DGs is necessary when the supply of renewable energy sources (RES) cannot keep up with the rising demand. Controllable DGs can improve the RES's performance in this manner. Installed RES capacity determines which controlled DG is most appropriate for a given situation. Diesel Engines (DEs) are considered to be hybrids in this study. In order to estimate the total generating cost of the hybrid DGs, the DE's generation cost is taken from [40]. RESs are swapped out for hybrid DGs in this scenario in order to see if there is a noticeable increase in performance. Replacement ensures that the hybrid DG provides 100 kW of power generation every day, regardless of the performance of the RES. Studies on the cost co-efficient of hybrid DG can be found in [42] and [43]. It's easier to compare the two possible combinations of DGs studied in the preceding example with hybrid DGs. The proposed method employs the same boundary conditions as the previous example.

Based on a 24-hour variable load, the implementation is designed to minimize bus voltage deviation while minimizing power loss. Variable load situations

AUTHOR C

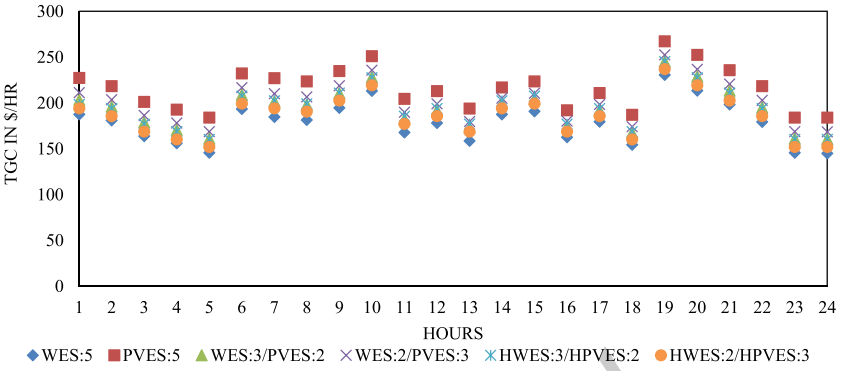


Fig. 12. Total generation cost under different configurations of microgrid.

ensure that the best compromise solution is found. To see if hybrid DGs really do provide a performance boost, researchers compared the data from all of the different scenarios. One of the most important benefits of using hybrid distributed generation (DG) on the grid is an increase in DG penetration. Because of increased penetration of DGs, the microgrid's performance has been enhanced. It is shown in Fig. 11 that over the course of a day, the final configuration achieved by the various examples loses power. It is best to replace RES with hybrid DGs, which have the lowest power loss at all times of day. Furthermore, even in the most ideal setups, the RES's low delivery performance renders all of the remaining situations pointless. Figure 12 compares the various scenarios' total production costs. An interconnected microgrid reduces the total generating cost significantly when using hybrid DGs. Hybrid WES costs less to produce than hybrid PVES, but this can be reversed for larger plants. A secondary objective of this research is to determine how to reduce the total cost of microgrid emissions while still addressing global warming concerns, which is impossible to do without using hybrid DGs.

5. Conclusion and future work

Reconfiguration and placement of DGs in the microgrid will be implemented simultaneously as part of the proposed work. The problem has been developed by taking into consideration two critical objectives: minimizing generation costs and minimizing voltage deviations. The operational constraints of the microgrid and DGs are considered when solving the optimization problem. Incorporating the principles of migrating and descending curves into MFO enhances its search capabilities. Heuristic fuzzy has been integrated to convert multi-objective optimization problems to single-objective optimization problems in conjunction with IMFO. The realistic characteristics of the microgrid and DGs are used in the analysis to make it more effective. In addition, four case studies examine the impact of PVES and WES integration into microgrids. Hybrid DGs were also studied for their potential to improve performance. The PVES and WES case studies yielded a slew of interesting findings. The investigation reveals that in order for the overall system generation cost and real power loss to be reduced, the number of WES customers has to increase. It cost 169.60 $/hr more to install and maintain WES than it did to run it, but transmission losses were cut by 41.33 % and bus voltage was raised to 0.9508 pu. Furthermore, it is clear from the simulation results that using this approach yields better results than using the current methods. In addition, the analysis looked at various combinations of DGs in order to find the best possible DG combination. The value of hybrid DGs over stand-alone DGs was realized most importantly. We can also compare the relative performance advantages of WES and PVES using the next day's predicted daily load curve and the predicted daily power generation curves for both systems. This study can make use of the seasonally variable annual anticipated power generation from WES and PVES. When non-linear loads are connected, the current research can be extended to consider power quality constraints.

References

[1] Zhao, Junhui, et al., A review of active management for distribution networks: current status and future development trends, *Electric Power Components and Systems* **42**(3-4) (2014), 280–293.

AUTHOR COPY

[2] Niknam, Taher and Abdollah Kavousi-Fard, Optimal energy management of smart renewable micro-grids in the reconfigurable systems using adaptive harmony search algorithm, *International Journal of Bio-Inspired Computation* **8**(3) (2016), 184–194.

[3] Gazijahani, Farhad Samadi and Javad Salehi, Stochastic multi-objective framework for optimal dynamic planning of interconnected microgrids, *IET Renewable Power Generation* **11**(14) (2017), 1749–1759.

[4] Wang, Zhaoyu, et al., Robust optimization based optimal DG placement in microgrids, *IEEE Transactions on Smart Grid* **5**(5) (2014), 2173–2182.

[5] Khorram-Nia, Reza, Bahman Bahmani-Firouzi and Mohsen Simab, Optimal switching in reconfigurable microgrids considering electric vehicles and renewable energy sources, *Journal of Renewable and Sustainable Energy* **10**(4) (2018), 045905.

[6] Daniel E. Olivares, et al., Trends in microgrid control, *IEEE Transactions on Smart Grid* **5**(4) (2014), 1905–1919.

[7] Abd El-salam, Mirna, Eman Beshr and Magdy Eteiba, A new hybrid technique for minimizing power losses in a distribution system by optimal sizing and siting of distributed generators with network reconfiguration, *Energies* **11**(12) (2018), 3351.

[8] Badran, Ola, et al., Optimal reconfiguration of distribution system connected with distributed generations: A review of different methodologies, *Renewable and Sustainable Energy Reviews* **73** (2017), 854–867.

[9] Jabbari-Sabet, Reza, Seyed-Masoud Moghaddas-Tafreshi and Seyed-Sattar Mirhoseini, Microgrid operation and management using probabilistic reconfiguration and unit commitment, *International Journal of Electrical Power & Energy Systems* **75** (2016), 328–336.

[10] Sedighizadeh, Mostafa, et al., Optimal distribution feeder reconfiguration and generation scheduling for microgrid day-ahead operation in the presence of electric vehicles considering uncertainties, *Journal of Energy Storage* **21** (2019), 58–71.

[11] Y.C. Huang, Enhanced-genetic-algorithm-based fuzzy multi-objective approach to distribution network reconfiguration, *IEE Proceedings-Generation, Transmission and Distribution* **149**(5) (2002), 615–620.

[12] Li, Yuanzheng, et al., Multi-objective optimal dispatch of microgrid under uncertainties via interval optimization, *IEEE Transactions on Smart Grid* **10**(2) (2017), 2046–2058.

[13] Li, Peng, et al., Stochastic optimal operation of microgrid based on chaotic binary particle swarm optimization, *IEEE Transactions on Smart Grid* **7**(1) (2015), 66–73.

[14] Niknam, Taher, Rasoul Azizipanah-Abarghooee and Mohammad Rasoul Narimani, An efficient scenario-based stochastic programming framework for multi-objective optimal micro-grid operation, *Applied Energy* **99** (2012), 455–470.

[15] M. Moghaddam, A. Kalam, J. Shi et al., A new model for reconfiguration and distributed generation allocation in distribution network considering power quality indices and network losses, *IEEE Systems Journal* **14**(3) (2020), 3530–3538.

[16] J. Li, P. Liu and Z. Li, Optimal design and techno-economic analysis of a solar-wind-biomass off-grid hybrid power system for remote rural electrification: A case study of west China, *Energy* **208** (2020), 1–12.

[17] M. Daneshvar, B. Mohammadi-Ivatloo, M. Abapour, S. Asadi and R. Khanjani, Distributionally robust chance-constrained transactive energy framework for coupled electrical and gas microgrids, *IEEE Trans Ind Electron* **68**(1) (2021), 347–357.

[18] A. Valencia, R.A. Hincapie and R.A. Gallego, Optimal location, selection, and operation of battery energy storage systems and renewable distributed generation in medium–low voltage distribution networks, *J Energy Storage* **34** (2021), Art. no. 102158. doi: 10.1016/j.est.2020.102158.

[19] M. Ahmadi, O.B. Adewuyi, M.S.S. Danish, P. Mandal, A. Yona and T. Senjyu, Optimum coordination of centralized and distributed renewable power generation incorporating battery storage system into the electric distribution network, *Int J Electr Power Energy Syst* **125** (2021), Art. no. 106458. doi: 10.1016/j.ijepes.2020.106458.

[20] M. Naguib, W.A. Omran and H.E. Talaat, Performance Enhancement of Distribution Systems via Distribution Network Reconfiguration and Distributed Generator Allocation Considering Uncertain Environment, *Journal of Modern Power Systems and Clean Energy* **10**(3) (2021), 647–655.

[21] L. Ge, H. Liu, J. Yan, X. Zhu, S. Zhang and Y. Li, Optimal Integrated Energy System Planning with DG Uncertainty Affine Model and Carbon Emissions Charges, *IEEE Transactions on Sustainable Energy* **13**(2) (2021), 905–918.

[22] H.A. Taha, M.H. Alham and H.K. Youssef, Multi-Objective Optimization for Optimal Allocation and Coordination of Wind and Solar DGs, BESSs and Capacitors in Presence of Demand Response, *IEEE Access* **10** (2022), 16225–16241.

[23] Gazijahani, Farhad Samadi and Javad Salehi, Robust design of microgrids with reconfigurable topology under severe uncertainty, *IEEE Transactions on Sustainable Energy* **9**(2) (2017), 559–569.

[24] Kavousi-Fard, Abdollah and Amin Khodaei, Efficient integration of plug-in electric vehicles via reconfigurable microgrids, *Energy* **111** (2016), 653–663.

[25] Dall'Anese, Emiliano and B. Georgios, Giannakis, Risk-constrained microgrid reconfiguration using group sparsity, *IEEE Transactions on Sustainable Energy* **5**(4) (2014), 1415–1425.

[26] Nikmehr, Nima, Sajad Najafi-Ravadanegh and Amin Khodaei, Probabilistic optimal scheduling of networked microgrids considering time-based demand response programs under uncertainty, *Applied Energy* **198** (2017), 267–279.

[27] Golshannavaz, Sajjad, Saeed Afsharnia and Pierluigi Siano, A comprehensive stochastic energy management system in reconfigurable microgrids, *International Journal of Energy Research* **40**(11) (2016), 1518–1531.

[28] M. Hemmati, et al., Risk-based optimal scheduling of reconfigurable smart renewable energy based microgrids, *International Journal of Electrical Power & Energy Systems* **101** (2018), 415–428.

[29] Maulik, Avirup and Debapriya Das, Optimal operation of a droop-controlled DCMG with generation and load uncertainties, *IET Generation, Transmission & Distribution* **12**(12) (2018), 2905–2917.

[30] Kanwar, Neeraj, et al., Optimal distributed resource planning for microgrids under uncertain environment, *IET Renewable Power Generation* **12**(2) (2017), 244–251.

[31] Nafisi, Hamed, et al., Optimal daily scheduling of reconfiguration based on minimisation of the cost of energy losses and switching operations in microgrids, *IET Generation, Transmission & Distribution* **9**(6) (2015), 513–522.

[32] Gaing, Zwe-Lee, Particle swarm optimization to solving the economic dispatch considering the generator constraints, *IEEE Transactions on Power Systems* **18**(3) (2003), 1187–1195.

AUTHOR COPY

[33] Bornapour, Mosayeb, et al., Optimal stochastic scheduling of CHP-PEMFC, WT, PV units and hydrogen storage in reconfigurable micro grids considering reliability enhancement, *Energy Conversion and Management* **150** (2017), 725–741.

[34] Chen, Changsong, et al., Smart energy management system for optimal microgrid economic operation, *IET Renewable Power Generation* **5**(3) (2011), 258–267.

[35] Mohammadi, Sirus, Soodabeh Soleymani and Babak Mozafari, Scenario-based stochastic operation management of microgrid including wind, photovoltaic, micro-turbine, fuel cell and energy storage devices, *International Journal of Electrical Power & Energy Systems* **54** (2014), 525–535.

[36] J. Jithendranath and Debapriya Das, Scenario-based multi-objective optimisation with loadability in islanded microgrids considering load and renewable generation uncertainties, *IET Renewable Power Generation* **13**(5) (2019), 785–800.

[37] Gazijahani, Farhad Samadi, Sajad Najafi Ravadanegh and Javad Salehi, Stochastic multi-objective model for optimal energy exchange optimization of networked microgrids with presence of renewable generation under risk-based strategies, *ISA Transactions* **73** (2018), 100–111.

[38] Hossam A. Gabbar and Aboelsood Zidan, Optimal scheduling of interconnected micro energy grids with multiple fuel options, *Sustainable Energy Grids and Networks* **7** (2016), 80–89.

[39] Chen, Jian, et al., Optimal sizing for grid-tied microgrids with consideration of joint optimization of planning and operation, *IEEE Transactions on Sustainable Energy* **9**(1) (2017), 237–248.

[40] Xiancheng Wang, Srinivasan Thiruvenkadam, Hyuntae Kim and In-ho Ra, Exploration of DG Placement Strategy of Microgrids via FMFO Algorithm: Considering Increasing Power Demand and Diverse DG Combinations, *Energies* **13** (2020), 6568; pp. 1–24. doi:10.3390/en13246568.

[41] S. Mirjalili, Moth-Flame Optimization Algorithm: A Novel Nature inspired Heuristic Paradigm, *Knowledge-Based Systems* **89** (2015), 228–249.

[42] Ed McKenna and Timothy L. Olsen, Performance and Economics of a Wind-Diesel Hybrid Energy System: Naval Air Landing Field, San Clemente Island, California, DOE Strategic Environmental Development Research Program, *National Renewable Energy Laboratory*, 1999.

[43] Peter Ozaveshe Oviroh and Tien-Chien Jen, The energy cost analysis of hybrid systems and Diesel Generators in powering selected base transceiver station locations in Nigeria, *Energies* **11** (2018), 687.

[44] P. Gangwar, S.N. Singh and S. Chakrabarti, Multi-objective planning model for multiphase distribution system under uncertainty considering reconfiguration, *IET Renew Power Gener* **13**(12) (2019), 2070–2083.

[45] S. Thiruvenkadam, H.-J. Kim and I.-H. Ra, Optimal Allocation of IaaS Cloud Resources through Enhanced Moth Flame Optimization (EMFO) Algorithm, *Electronics* **11** (2022), 1095. https://doi.org/10.3390/electronics11071095

AUTHOR COPY